

DAMAGE CLASSIFICATION OF URBAN AREAS IN THE 2016 KUMAMOTO EARTHQUAKE USING TEXTURE MEASURES FROM ALOS-2 PALSAR-2 IMAGES

Homa Zakeri^{1*}, Fumio Yamazaki¹ and Wen Liu¹

¹ Department of Urban Environment Systems, Chiba University, Chiba 263-8522, Japan

* Correspondence: homa.zakeri@chiba-u.jp

ABSTRACT: After a natural disaster strikes, it is necessary to assess the amount of damage in vulnerable areas immediately. Synthetic aperture radar (SAR) is independent of time and weather conditions for capturing images of ground surface. In this research, post-event polarized data from ALOS-2 PALSAR-2 with 3.12-m resolution were used to classify the damaged areas in Mashiki town, Kumamoto prefecture, Japan, which was severely affected by the April 14, 2016 (Mw6.2) earthquake and the April 16, 2016 (Mw7.0). Accordingly, the texture measures of the SAR backscatter data set were prepared and used for supervised classification using the Support Vector Machine (SVM) algorithm. This study aims to explore the potential of texture features for detecting damaged regions after earthquakes.

KEY WORDS: damage assessment, classification, texture measures, the 2016 Kumamoto earthquake, SVM

1. INTRODUCTION

Remote sensing is an efficient tool to obtain a wide range of information of the earth surface when a natural disaster strikes. Damage assessment of buildings immediately after the occurrence of a natural disaster is one of the most important topics of satellite remote sensing. Significant amount of studies (Yamazaki et al. 2005; Miura et al. 2013) have been conducted to monitor damage condition in urban areas.

An Mw6.2 earthquake hit the Kumamoto prefecture in Kyushu Island, Japan on April 14, 2016. Twenty-eight (28) hours later, another earthquake of Mw7.0 occurred at a close location to the first event (USGS, 2016; JMA, 2016). Extensive landslide and damage to buildings, roads and bridges were associated and human casualties had been reported including 50 deaths by the Kumamoto earthquake (Cabinet Office of Japan, 2016). The epicenters of the both events were located in Mashiki town (about 33 thousand-population), to the east of Kumamoto city (about 735 thousand-pop.). Mashiki town was most severely affected due to very strong seismic ground motion (Hata et al., 2016). A continuous surface faulting was observed in the agricultural field (Yamazaki and Liu, 2016) and the coseismic displacements were evaluated from LiDAR data (Moya et al., 2017) in the town.

This paper evaluates the use of texture analysis from a HH and HV polarized ALOS-2 PALSAR-2 image taken after the 2016 Kumamoto earthquake for detecting building damage in Mashiki town. Support Vector Machine (SVM) algorithm was used for supervised classification of the study area in four land-cover classes: damaged urban, non-damaged urban, vegetation, and paddy field. The result was compared visually with the damage grades of built-up areas, prepared by the field surveys of the Architectural Institute of Japan (AIJ), (NILIM, 2016).

2. STUDY AREA AND DATA SET

The study area is the central part of Mashiki town, Kumamoto prefecture, Japan (shown as yellow frame in Figure 1), which is closely located the Futagawa fault. The black square in Figure 2(a) shows the study area, located between the Mashiki Town Hall building and Akitsu River with a building-collapse ratio of more than 50%. This area was used for preparing a land-cover classification map in this study. The damage grades of built-up areas (with 2,340 buildings) prepared by AIJ are represented by collapsed building ratio in a 57 m x 57 m grid-cell.

A post-event PALSAR-2 image taken April 21, 2016 was used for the texture analysis. Figure 2(b) shows a color composite of the HH, HV, HH-HV polarizations. The study area includes built-up urban, vegetation, and paddy field. The SAR image was taken in the ascending path with right-look. The data product is Level 1.5. The off-nadir angle was 30.4 degrees at the center of the image and the azimuth and range resolution was 3.12 m. The image was taken with the full polarization (HH, HV, VV, and VH) in the StripMap2 mode. In this study, only HH and HV polarizations were used considering the sensitivity of them for detecting built-up and vegetation areas. Pre-processing was done by converting the digital number of the data set to backscattering coefficient (sigma-naught in dB) using the equation below (JAXA, 2016).

$$\sigma^0 = 10.0 \log_{10}(DN^2) + CF_1 \quad (1)$$

where DN is the digital number of backscattering intensity, CF_1 is the calibration factor, and θ_{loc} is the local incidence angle. Then Lee filter with the window size 3x3 was applied to reduce speckle noise.

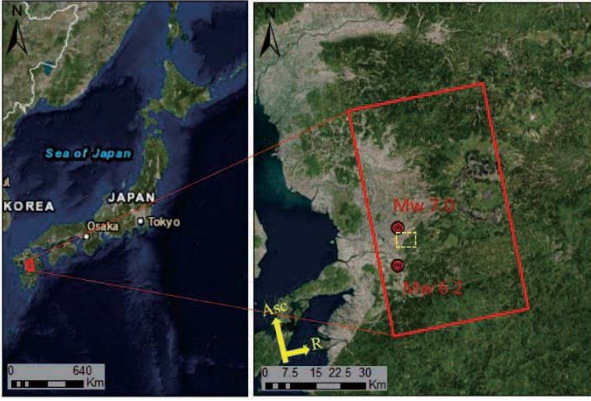
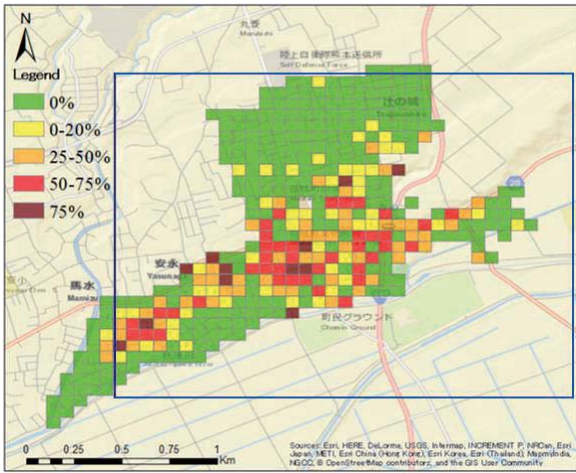
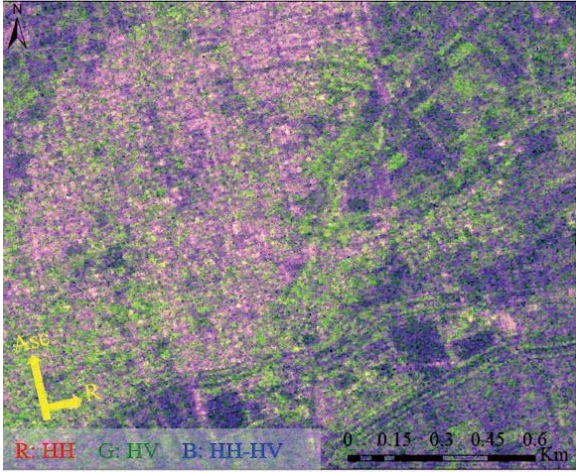


Figure 1. Location of ALOS-2 image used in this study.



(a)



(b)

Figure 2. (a) Building-collapse map, prepared according to the field surveys (NILIM, 2016); (b) the color composite of the post-event SAR backscattering coefficient image. Dark blue border in (a) represents the location of (b) in Mashiki town.

3. METHODOLOGY

After performing the pre-processing steps, texture measures were calculated for the backscattering coefficients of HH and HV. Previous researches have

shown that the texture measures provide vital information from radar imagery (Dell'Acqua et al., 2003; Ulaby et al., 1982). Among several statistical texture methods, the grey-level co-occurrence matrix (GLCM) algorithm is one of the most powerful methods for land-cover monitoring (Haralic et al., 1973), and thus, the GLCM is used in this study.

Texture represents the spatial distribution of the grey-level value and its frequency with another one under a specific displacement and orientation. Different features such as *angular second moment*, *contrast*, *correlation*, *homogeneity*, *variance*, *mean*, *entropy*, *energy*, *maximum probability* and *dissimilarity* were extracted from the GLCM using a specific window-size by the following equations:

$$\text{Angular Second Moment} = \sum_i \sum_j \{P(i, j)\}^2 \quad (2)$$

$$\text{Contrast} = \sum_{n=0}^{N_g-1} n^2 \left\{ \sum_{i=1}^{N_g} \sum_{j=1}^{N_g} P(i, j) \right\}_{|i-j|=n} \quad (3)$$

$$\text{Correlation} = \frac{\sum_i \sum_j (ij)P(i, j) - \mu_x - \mu_y}{\sigma_x \sigma_y} \quad (4)$$

$$\text{Homogeneity} = \sum_i \sum_j \frac{1}{1 + (i - j)^2} P(i, j) \quad (5)$$

$$\text{Variance} = \sum_i \sum_j (i - \mu)^2 P(i, j) \quad (6)$$

$$\text{Mean} = \sum_{i=2}^{2N_g} i p_{x+y}(i) \quad (7)$$

$$\text{Entropy} = - \sum_i P \log(P(i, j)) \quad (8)$$

$$\text{Dissimilarity} = \sum_{i,j=0}^{N_g-1} P_{i,j} (-\ln P_{i,j}) \quad (9)$$

where $p(i, j)$ is the (i, j) -th entry in a normalized grey-tone spatial dependence matrix $P(i, j)/R$; R is the total sum of P ;

$p_x(i) = \sum_{j=1}^{N_g} P(i, j)$ is the i -th entry in the

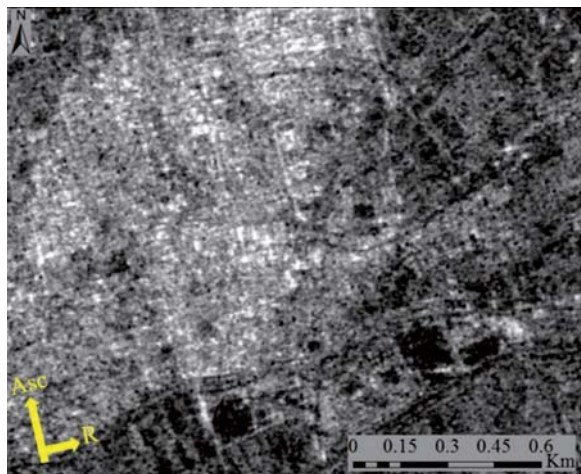
marginal probability matrix obtained by summing the rows of $p(i, j)$; and μ_x , μ_y , σ_x and σ_y are the means and standard deviations of p_x and p_y .

In this study, eight textural features at angle 0° and distance 1, and window size 3×3 and a quantization level 64 were used to evaluate its performance for classification.

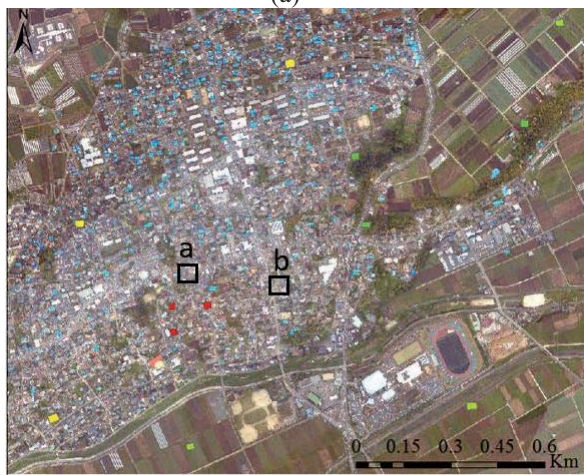
In order to use more effective texture measures for classification, the statistics information such as the minimum, mean, maximum, and standard deviation of

pixels values for each damage ratio class by AIJ were evaluated. It was observed that only in the mean texture data differences among the damage grades were observed. Therefore, the mean texture of HH, shown in Figure 3(a), and that of HV were selected to stack with the original values of HH and HV as the input data set for classification. Supervised classification is applied to detect the damaged areas. The support vector machine (SVM) algorithm (Vanpik, 2000) was chosen for this purpose.

A closed-up of the aerial photograph taken at 12:21 (local time) on April 16, 2018 by the Geospatial information Authority of Japan (GSI) was used to select training samples for classification. The training samples mainly consist of square shapes of 30 m in length, as shown in Figure 3(b) and three sample areas were selected for each class.



(a)



(b)

Figure 3. (a) Mean measure of texture analysis from post-event image; (b) training samples used for classification plotted on the aerial photograph of central Mashiki town taken on April 16, 2016 by GSI. The black frames a, and b in (b) show the location of classification result examples in Figure 4.

4. RESULTS

Four land-covers classes: damaged urban, non-damaged urban, vegetation and paddy fields were considered in the supervised classification based on SVM algorithm. Since training samples have an important role in supervised classification, we examine different size of them. It was observed that each sample is better to include one individual building in cases of damaged and non-damaged classes. Thus, the same size and square shape were considered. Therefore, the same number of pixels was used for all the four classes in classification. Moreover, the damaged samples were selected from collapsed building areas, not from debris. The result of classification is shown in Figure 4.

For validating the result of classification, we compared them visually with an aggregated damage-grade map by NILIM (2016). The areas shown in Figure 4 contain the damage grade more than 50% based on the report. We used the footprint of buildings provided by the Geospatial Information Authority of Japan (GSI) to make ground truth data by visual inspection and having more precise comparison with the NILIM map. The red and yellow footprints show damaged and non-damaged buildings in the target area. The comparison between truth data (left) and classification results (right) show similarity for damaged parts and non-damaged buildings to some extent. However, a more detailed comparison is needed in the future.



(a)



(b)

Figure 4. Aerial images with building footprints (left). Red and yellow polygons were made by the authors showing damaged and non-damaged buildings. Classification results using SVM algorithm (right). The location of (a) and (b) are shown in Figure 3(b).

5. CONCLUSIONS

In this study, the GLCM texture measures were applied to improve the supervised classification of SAR intensity images to detect damage parts of urban areas. Mashiki town, Kumamoto prefecture, Japan, which was most severely affected by the April 2016 Kumamoto earthquake was selected as a study area. By comparing the minimum, mean, maximum and standard deviation of pixel values of eight texture measures in each polarization with the damage-grade map prepared by NILIM, the mean texture was found to show a difference among damage levels of built-up areas. Therefore, the mean textures of the HH and HV polarization images and their original values were used for SVM classification of the target area. The classification was carried out for four classes: damaged urban, non-damaged urban, vegetation, paddy fields. The result was compared with the damage-ratio map by the field survey. Through the comparison, the classification result from the SAR data was found to be consistent with the field survey result.

ACKNOWLEDGMENT

The ALOS-2 PALSAR-2 data used in this study are owned by the Japan Aerospace Exploration Agency (JAXA) and were provided through the JAXA's ALOS-2 research program (RA4, PI No. 1503).

REFERENCES

- ALOS Research and Application Project of EPRC, JAXA http://www.eorc.jaxa.jp/ALOS2/en/calval/calval_index.htm
- Cabinet Office of Japan. 2016. Summary of damage situation in the Kumamoto earthquake sequence. <http://www.gsi.go.jp/BOUSAI/H27-kumamoto-earthquake-index.html>
- Dell'Acqua, F., Gamba, P., 2003. Texture-base characterization of urban environmental on satellite SAR images. *IEEE Transactions on Geoscience and Remote Sensing*, 41(1), pp. 153–159.
- Geospatial Information Authority of Japan (GSI), 2016. <http://fgd.gsi.go.jp/download/menu.php>
- Haralick, R. M., Shanmugan, K., Dinstein, I., 1973. Texture feature for image classification. *IEEE Transactions on Systems, Man and Cybernetics*, SMC-3, No. 6, pp. 610-621.
- Hata, Y., Goto, H., and Yoshimi, M., 2016. Preliminary analysis of strong ground motions in the heavily damaged zone in Mashiki town, Kumamoto, Japan, during the mainshock of the 2016 Kumamoto earthquake (Mw 7.0) observed by a dense seismic array. *Seismological Research Letters*, Vol. 87, No. 5.
- Japan Meteorological Agency (JMA), 2016. http://www.jma.go.jp/jma/en/2016_Kumamoto_Earthquake/2016_Kumamoto_Earthquake.html
- Miura H., Midorikawa S., Kerle N., 2013. Detection of building damage areas of the 2006 Central Java Indonesia Earthquake through digital analysis of optical satellite images. *Earthquake Spectra*, Vol. 29, No. 2, pp. 453-473.
- Moya L., Yamazaki F., Liu W., Chiba T., 2017. Calculation of coseismic displacement from Lidar data in the 2016 Kumamoto, Japan, earthquake. *Natural Hazards and Earth System Sciences, European Geosciences Union*, Vol. 17, pp.143-156.
- National Institute for Land and Infrastructure Management (NILIM), Quick report of the field survey on the building damage by the 2016 Kumamoto earthquake. Technical Note No. 929.
- Ulaby, F. T., R. K. Moore, and A.K. Fung, 1982. *Microwave Remote Sensing: Active and Passive*, Vol. II -- Radar Remote Sensing and Surface Scattering and Emission Theory, Addison-Wesley, Advanced Book Program, Reading, Massachusetts.
- United States Geological Survey (USGS), 2016. <https://earthquake.usgs.gov/earthquakes/eventpage/us20005iis#executive>
- Vapnik, V., 2000. *The Nature of Statistical Learning Theory*. Springer, New York, NY, USA.
- Yamazaki, F., Yano, Y., and Matsuoka, M., 2005. Visual damage interpretation of building in Bam city using QuickBird images following the 2003 Bam, Iran. *earthquake. Earthquake Spectra*, Vol. 21, No. S1, pp. 329-336.
- Yamazaki, F., and Liu, W., 2016. Remote sensing technologies for post-earthquake damage assessment: A case study on the 2016 Kumamoto earthquake. *6th Asia Conference on Earthquake Engineering*, 13p.